



Published in final edited form as:

Dev Biol. 2012 August 15; 368(2): 382–392. doi:10.1016/j.ydbio.2012.06.008.

Forward genetics uncovers Transmembrane protein 107 as a novel factor required for ciliogenesis and Sonic Hedgehog signaling

Kasey J. Christopher¹, Baolin Wang², Yong Kong^{3,4}, and Scott D. Weatherbee^{1,*}

¹Department of Genetics, Yale University, New Haven, CT 06520

²Department of Genetics, Weill Medical College of Cornell University, New York, NY 10021

³Department of Molecular Biophysics and Biochemistry, Yale University, New Haven, CT 06520

⁴W.M. Keck Foundation Biotechnology Resource Laboratory, Yale University, New Haven, CT 06520

Abstract

Cilia are dynamic organelles that are essential for a vast array of developmental patterning events, including left-right specification, skeletal formation, neural development, and organogenesis. Despite recent advances in understanding cilia form and function, many key ciliogenesis components have yet to be identified. By using a forward genetics approach, we isolated a novel mutant allele (*schlei*) of the mouse *Transmembrane protein 107* (*Tmem107*) gene, which we show here is critical for cilia formation and embryonic patterning. *Tmem107* is required for normal Sonic hedgehog (Shh) signaling in the neural tube and acts in combination with Gli2 and Gli3 to pattern ventral and intermediate neuronal cell types. *schlei* mutants also form extra digits, and we demonstrate that *Tmem107* acts in the Shh pathway to determine digit number, but not identity, by regulating a subset of Shh target genes. Phenotypically, *schlei* mutants share several features with other cilia mutants; however, spatial restriction of mutant phenotypes and lack of left-right patterning defects in *schlei* animals suggest differential requirements for *Tmem107* in cilia formation in distinct tissues. Also, in contrast to mutants with complete loss of cilia, *schlei* mutants retain some function of both Gli activator and repressor forms. Together, these studies identify a previously unknown regulator of ciliogenesis and provide insight into how ciliary factors affect Shh signaling and cilia biogenesis in distinct tissues.

Keywords

cilia; Sonic hedgehog (Shh); limb; neural tube; mouse; forward genetics; *Tmem107*

INTRODUCTION

The molecular nature of several human diseases including Nephronophthisis, Joubert syndrome, Bardet-Biedl Syndrome, Oral-Facial-Digital Syndrome 1, and Meckel Syndrome

© 2012 Elsevier Inc. All rights reserved

*Corresponding author.

Publisher's Disclaimer: This is a PDF file of an unedited manuscript that has been accepted for publication. As a service to our customers we are providing this early version of the manuscript. The manuscript will undergo copyediting, typesetting, and review of the resulting proof before it is published in its final citable form. Please note that during the production process errors may be discovered which could affect the content, and all legal disclaimers that apply to the journal pertain.

has been linked to defects in the development, morphology, or function of a small cellular organelle called the cilium (Fliegauf et al., 2007; Sharma et al., 2008; Nigg and Raff, 2009). Cilia are microtubule-based extensions of the cell surrounded by a membrane that is contiguous with, but distinct from, the plasma membrane. They largely fall into two distinct classes: motile cilia, which are thought to function by generating flow in structures such as the embryonic node, lung and the fallopian tubes, and non-motile primary cilia, whose function is less well-defined. What is known is that primary cilia are found on nearly all cells of the vertebrate embryo and in recent years have been shown to play a striking role in a vast array of developmental patterning events, including skeletal formation, the establishment of left-right asymmetry, and organogenesis (Goetz and Anderson, 2010). Long overlooked, cilia have recently emerged as key organelles not only for studying human disease, but also for understanding developmental pathways in many animals. Importantly, primary cilia have recently been implicated in the regulation of several key developmental signaling pathways, the best studied of which is Hedgehog (Hh) signaling (Huangfu et al., 2003; Haycraft et al., 2005; Huangfu and Anderson, 2005; Liu et al., 2005).

Hh acts through a conserved signaling cascade to regulate the development of multiple organs including the eyes, lungs, and limbs. Binding of Hh ligands to their transmembrane receptor Patched (Ptch) relieves Ptch-mediated inhibition of the transmembrane protein Smoothed (Smo), allowing Smo to translocate into the cilium and activate the pathway (Ingham and McMahon, 2001; Rohatgi et al., 2007). Smo acts through an as yet unclear mechanism to modulate the activities of the Gli proteins, which are the transcriptional effectors of Hh signaling. Gli1 is a transcriptional activator, while Gli2 and Gli3 can act as both activators and repressors (Dai et al., 1999; Sasaki et al., 1999). In the absence of the ligand, Gli3 and Gli2 are proteolytically processed into cleaved repressor forms (GliR), but binding of Hh to Ptch and subsequent Smo derepression prevents efficient processing so that the full-length, activator form (GliA) predominates (Wang et al., 2000; Ingham and McMahon, 2001; Pan et al., 2009), resulting in the transcription of Hh target genes.

In vertebrates, primary cilia are required for both positive and negative regulation of the Hh pathway. Both the processing and activation of full-length Gli proteins requires functional cilia (Haycraft et al., 2005; Huangfu and Anderson, 2005; Liu et al., 2005). Sonic hedgehog (Shh), one of three vertebrate Hh homologues, plays a crucial role in the patterning and morphogenesis of a variety of tissues and organs (Ribes and Briscoe, 2009; Traiffort et al., 2010; Harfe, 2011). In the limb, Shh is expressed in a region of the posterior mesenchyme and is required to determine the number and identity of the digits (Riddle et al., 1993; Chiang et al., 2001). In the neural tube, Shh specifies distinct neuronal types in a concentration-dependent manner (Roelink et al., 1994; Tanabe et al., 1995). Mutations that result in near-complete absence of cilia, such as *IFT88^{null}* or *IFT172^{wim}*, cause Shh signaling-related defects in the neural tube and limb, including the loss of ventral neuronal cell types and severe polydactyly (Huangfu et al., 2003; Haycraft et al., 2007). Despite an increasing understanding of the relationship between cilia and Shh, many of the components that are required to build cilia and promote Shh signaling during development are unknown.

Through a forward genetics screen, we identified a novel mouse mutant *schlei* that displays Shh-related defects including preaxial polydactyly, exencephaly, and disrupted ventral neural tube patterning. These phenotypes are also hallmarks of defective cilia, and we show that *schlei* mutants have decreased numbers of cilia in several developing tissues and organs. By employing new high-throughput sequencing technologies, we demonstrate that the *schlei* phenotype results from a point mutation in *Tmem107*, a gene encoding a previously uncharacterized transmembrane protein. We find that *Tmem107* acts synergistically with Gli2 as a positive mediator of Shh to specify ventral neuronal cell types, and also acts negatively in combination with Gli3 to constrain the dorsal expansion of intermediate-level

neuronal cells. Additionally, *Tmem107* functions in the limb to control digit number, but not digit identity, through differential regulation of distinct target genes of the *Shh* pathway. The effects of *Tmem107* on developmental patterning underline the importance of fully functional cilia in *Shh* signaling. Further, these studies demonstrate the increasing ease and utility of forward genetics screens in the mouse as advances in high-throughput sequencing technologies facilitate the identification of causative mutations.

MATERIAL AND METHODS

Mouse Strains

Mutant lines used included *Ptch1^{tm1Mps}* (Goodrich et al., 1997), *Gli3^{XT-J}* (Hui and Joyner, 1993), *Smo^{bnb}* (Casparly et al., 2002), *Gli2^{tm2.1Alj}* (Bai and Joyner, 2001), and *Shh^{tm1Chg}* (Chiang et al., 1996). Mutant alleles were genotyped as previously described.

Generation and Mapping of *schlei*

Initial mapping of the *schlei* mutation utilized two to five simple sequence length polymorphism markers per chromosome to identify linkage between the polydactyly phenotype and C57BL/6J DNA polymorphisms. *schlei* was linked to Chromosome 11 and the *schlei* interval was subsequently narrowed to between markers rs26892691 (68.06 Mb) and D11Mit320 (70.7 Mb). The *schlei* mutation has been crossed >11 generations onto the C3HeB/FeJ background, which removed more than 99.9% of the original mutagenized C57BL/6J background, supporting the idea that the *schlei* phenotype is monogenic. Mutant characterization was carried out at various stages of crossing into the C3HeB/FeJ background.

Sequence Capture

A Nimblegen mouse Sequence Capture 385K array was designed to contain oligos complementary to the *schlei* genomic locus (Chr11:68,058,821-70,766,988 Mb), minus repetitive sequences. Genomic DNA from an e11.5 *schlei* homozygote was isolated and then sheared by sonication, and adaptors were ligated to the resulting fragments. The adaptor-ligated templates were fractionated by agarose gel electrophoresis and fragments of the desired size were excised. Extracted DNA was amplified by ligation-mediated PCR, purified, and hybridized to the Sequence Capture array. The array was washed, and bound DNA was eluted, purified, and amplified by ligation-mediated PCR (similar to methods employed in (Choi et al., 2009)). The capture and sequencing experiments were performed at the W.M. Keck Foundation for Biotechnology Resources at Yale. This array also contained sequences from Chromosomes 4 & 7, unrelated to the *schlei* locus. For details about these sequences, please contact the authors.

Sequencing and Mutation Analysis

Captured libraries were sequenced on an Illumina Genome Analyzer II as single-end, 75-bp reads as previously described (Choi et al., 2009). Illumina reads were first trimmed based on their quality scores to remove low-quality regions using the program Btrim (Kong, 2011). A cutoff of 20 for average quality scores within a moving window of size 5-bp was used. Minimum acceptable read length was 25-bp. Other parameters of Btrim were set to defaults. The pre-processed reads were then aligned to the mouse genome reference sequence (mm9) using mapping program BWA (Li and Durbin, 2009). The mapping results were converted into SAMtools pileup format using SAMtools programs (Li et al., 2009). PCR duplicates were removed using the rmdup command from SAMtools. Single nucleotide variations (SNVs) were called using SAMtools' pileup command. Further filtering was performed using in-house scripts to exclude those SNV calls that had less than 3 reads or a SNP score

less than 20. Annotation was added based on the UCSC RefSeq gene model ((Pruitt et al., 2009); <http://genome.ucsc.edu/>).

Obtaining a Second *Tmem107* Allele

Generation of the *Tmem107^{tm1Lex}* allele was previously described (Tang et al., 2010). Cryopreserved sperm from the B6N.129S5-*Tmem107tm1Lex/Mmcd* strain (identification number 032632-UCD) was obtained from the Mutant Mouse Regional Resource Center, a NCRP-NIH funded strain repository, and was donated to the MMRRRC by Genentech, Inc. *Tmem107^{tm1Lex}* mice were generated via *in vitro* fertilization by Yale Animal Genomics Services and maintained on a C57Bl/6N background.

Expression Analysis

In situ hybridizations and immunofluorescence analyses were performed using standard methods (Nagy et al., 2003). Monoclonal antibodies that recognize Pax7, Pax6, Nkx6.1, Nkx2.2, and Shh were obtained from the Developmental Studies Hybridoma Bank developed under the auspices of the NICHD and maintained by the Department of Biological Sciences, The University of Iowa (Iowa City, IA, USA). Additional antibodies used included Olig2 (Millipore, Billerica, MA, USA), acetylated α -tubulin (Sigma-Aldrich, St. Louis, MO, USA), γ -tubulin (Sigma-Aldrich), and Arl13b (gift from Tamara Caspary, Atlanta, GA, USA; (Caspary et al., 2007)).

Skeletal Staining

Skeletons were prepared and stained with Alcian blue and Alizarin red using standard methods (Nagy et al., 2003).

Scanning Electron Microscopy

SEM was performed on open-face preparations of e10.5 neural tubes following standard methods through the Yale Center for Cellular and Molecular Imaging.

Cell Culture

Mouse embryonic fibroblasts (MEFs) were derived using standard methods (Nagy et al., 2003). MEFs were maintained in a 1:1 mix of DMEM:DMEM/F12 + 10% fetal bovine serum (FBS). For cilia staining, cells were plated on coverslips, grown to confluence, and starved for 72 hours in DMEM:DMEM/F12 containing 0.5% FBS.

RESULTS

schlei mutants display cilia defects

We performed an *N*-ethyl *N*-nitrosourea (ENU) screen for recessive mouse mutants at embryonic day (e) 12.5 (similar to (Kasarskis et al., 1998; Weatherbee et al., 2009)) and isolated the *schlei* mutant based on several characteristics including broadening of the limbs along the anteroposterior axis (Fig. 1A,B). This broadening resolved into preaxial polydactyly at later stages, with most mutant limbs showing at least one ectopic digit (n=23/27 limbs; Fig. 1C,D). Additional features of the *schlei* mutant phenotype included partially penetrant exencephaly (bracket in Fig. 1B), microphthalmia (arrowhead in Fig. 1B) and skeletal defects (see Fig. S1 in supplementary material), which together phenocopied mutants with abnormal primary cilia (Fliegau et al., 2007; Goetz and Anderson, 2010). To test whether cilia defects were the proximal cause of the *schlei* mutant phenotype, we performed immunofluorescence analysis for ciliary markers Arl13b and acetylated α -tubulin. We observed reduced numbers of cilia in *schlei* mutant limb mesenchyme and lining the lumen of the neural tube based on Arl13b staining (Fig. 1E-H). To confirm the

cilia phenotype in the neural tube, we performed scanning electron microscopy (SEM) in the lumen of e10.5 neural tubes. Consistent with Arl13b staining, there was a reduction in the number of cilia lining the *schlei* neural tube (Fig. 1I,J). In addition, we observed cilia with bulges (red arrowhead in Fig. 1J), long, curled cilia (red arrow in Fig. 1J), and abnormally thin cilia (yellow arrowhead in Fig. 1J) in *schlei* neural tubes.

We quantified the defect in cilia number using mouse embryonic fibroblasts (MEFs) and found that 59.14% of wild type cells formed cilia (arrowheads in Fig. 1K,L), compared to only 30.22% of mutant cells based on acetylated α -tubulin staining ($p=0.00045$ by two-tailed student's t-test with equal variances; $n=4$ cell lines; Fig. 1M). Despite the striking reduction of cilia number in MEFs and the neural tube, not all tissues were equally affected; *schlei* mutants did not develop left-right patterning defects, and correspondingly, cilia in the embryonic node appeared normal by SEM (data not shown and see Fig. S2 in supplementary material). In addition, *schlei* mutant kidneys and livers did not display obvious cysts by e18.5 (see Fig. S2 in supplementary material and data not shown). Cilia defects in several, but not all, embryonic tissues suggest that the *Schlei* gene product is a key component required for ciliogenesis and that it may play a role in the biogenesis or maintenance of specific types of cilia.

Gain and loss of Shh responsiveness in *schlei* mutant neural tubes

When cilia are lost, neural tube patterning reflects a diminished response to Shh signaling (Huangfu et al., 2003; Huangfu and Anderson, 2005; Liu et al., 2005; May et al., 2005; Houde et al., 2006). To test if the reduced cilia number in *schlei* neural tubes affected Shh signaling, we examined Shh-specified neuronal subtypes at e10.5. Despite the presence of Shh protein in the notochord, we observed multiple defects in ventral neuronal specification. The number of floorplate cells (Shh+, FoxA2+), which require the highest level of Shh signaling, was dramatically reduced in the cervical and limb regions of *schlei* mutant neural tubes (Fig. 2A,B; data not shown). V3 interneuron progenitors (Nkx2.2+), which require the next highest level of Shh signaling, were also reduced in number and located more ventrally in *schlei* neural tubes (Fig. 2C,D). Motor neuron progenitors (Olig2+) were specified in more medial and ventral locations, including the midline (Fig. 2E,F). These data are consistent with a reduced response to Shh signaling.

However, the *schlei* phenotype departs from most other cilia mutants in that the Olig2+ domain was also expanded dorsally, suggestive of a broader region of intermediate-level Shh signaling (bracket in Fig. 2F). Nkx6.1 marks a broad population of ventral neuronal progenitors and its dorsal expansion in *schlei* mutants indicates that V2 interneurons (Nkx6.1+; Olig2-) were also specified further from the Shh source (Fig. 2G,H and data not shown). Markers for dorsal cell fates, which are normally repressed by Shh, were either unchanged (Pax7+; Fig. 2I,J) or expanded ventrally (Pax6+; Fig. 2K,L). Overall, these data demonstrate that the *schlei* mutation is required for the highest-level response to Shh, presumably due to the loss of cilia in the mutant. However, *schlei* also displays features of other cilia mutants (ex. Arl13b^{hnn}, Mks1^{krc}), in which intermediate Shh targets expand dorsally (Casparly et al., 2007; Weatherbee et al., 2009). Furthermore, the borders of interneuron populations break down and we observed intermingling of different neuronal types (data not shown). Interestingly, *Shh* expression, which appeared normal in the notochord, was variably lost in gaps from the floorplate, particularly at the cervical and forelimb level, further supporting the hypothesis that there are differential regional requirements for the *Schlei* gene product (Fig. 2M,N).

The *schlei* mutation affects Shh signaling downstream of *Ptch1* in the neural tube

To determine how *schlei* affects Shh signaling in neuronal specification, we examined e10.5 embryos doubly homozygous for *schlei* and mutations in *Ptch1*, *Shh* or *Smo*. *Ptch1* acts negatively within the pathway and thus *Ptch1* mutants have constitutively active Shh signaling, which ventralizes the neural tube (Goodrich et al., 1997). Strikingly, loss of *schlei* resulted in a significant rescue of the *Ptch1* phenotype. Gross morphology in double mutant embryos was partially restored, including head formation, embryo size and neural tube closure (see Fig. S3 in supplementary material). In the neural tube, dorsal cell types (Pax6+) lost in *Ptch1* were restored in the double mutant, whereas ventral cell types such as motor neurons, V3 interneurons and floorplate cells were better restricted to a ventral domain than in *Ptch1* mutants (Fig. 3A,B). These results indicate that the *schlei* mutation exerts its effects downstream of *Ptch1* to restrict ventral neuronal cell type specification.

The expansion of intermediate Shh targets in *schlei* mutants suggested that the *schlei* mutation may also promote their specification. To test this, we analyzed the effect of the *schlei* mutation in *Shh* and *Smo* mutant backgrounds. As *Smo* is required for all Hh signaling, *Smo* mutant neural tubes are dorsalized, with a complete absence of Shh-dependent ventral cell types (Wijgerde et al., 2002). The most ventral cell types (floorplate, V3) were absent in both *Smo* and *schlei-Smo* mutants (Fig. 3C,D). However, in embryos doubly mutant for *schlei* and *Smo*, some Shh-specified cell types, including V2 interneurons and motor neurons, were able to form, but were intermingled with dorsal neurons, indicating that loss of *schlei* could rescue ventral neuron specification, but not regional restriction in *Smo* embryos (Fig. 3D). We observed similar results with *schlei-Shh* double mutants (Fig. 3E,F). Taken together, our analyses of embryos doubly mutant for *schlei* and components of the Shh pathway show that the *Schlei* gene product exerts its function downstream of Shh, *Ptch1*, and *Smo*. These results suggest that the *schlei* phenotype is the result not only of a loss of positive Shh function, but that the *Schlei* gene product can also specify neuronal identities independent of Shh ligand. Previous work has demonstrated that in the absence of *shh*, reduction of *Gli3* levels can result in a rescue of some Shh-dependent cell types (Litingtung and Chiang, 2000), similar to what we observed in the *schlei-Shh* double mutant. Thus, to determine whether the function of Gli transcription factors in the neural tube was altered in *schlei*, we examined *schlei-Gli2* and *schlei-Gli3* embryos.

Schlei acts in combination with *Gli2* and *Gli3* to pattern the ventral and intermediate neural tube

Our results suggested that *schlei* plays both a positive and negative role in Shh signaling in the neural tube. The Gli transcription factors also have dual roles in Shh-mediated neuronal specification. *Gli2* is the predominant transcriptional activator downstream of Shh signaling in the ventral neural tube, and is required to specify ventral cell types such as floorplate and V3 interneurons. *Gli2* mutants fail to form a floorplate, while V3 interneurons and motor neuron progenitors are specified more ventrally than in wild type ((Ding et al., 1998; Matise et al., 1998); Fig. 4A). We observed a synergistic effect in *schlei-Gli2* double mutants; in addition to the loss of floorplate cells, V3 interneurons were also completely absent (Fig. 4B). This suggests that while both *Gli2* and *Schlei* are required for floorplate specification, the two genes are redundantly required for V3 specification. *schlei-Gli2* embryos showed the ventral expansion of Pax6+ cells characteristic of *schlei* mutants (Fig. 4B). But strikingly, loss of *Gli2* blocked the dorsal expansion of V2 interneuron progenitors and motor neuron progenitors (Fig. 4B) normally observed in *schlei* mutants, indicating that *Gli2* is required for the ectopic activation of intermediate-level Shh targets.

In the neural tube, *Gli3* acts primarily as a repressor and affects the specification of medially located cell populations such as V0 interneurons, but is not required in the most ventral parts

of the neural tube ((Persson et al., 2002); Fig. 4C). Intriguingly, loss of *Gli3* greatly exacerbated the dorsal expansion of motor neuron progenitors and V2 interneuron progenitors observed in *schlei* (Fig. 4D). Correspondingly, the Pax6+ domain is restricted to a more dorsal region in the *schlei-Gli3* double mutant as compared to controls or the *schlei* single mutant (Fig. 4D). More ventrally, *schlei-Gli3* embryos showed loss of floorplate cells similar to *schlei* mutants, but also a dorsal expansion of V3 interneuron progenitors (Fig. 4D). Thus, our data indicate that Gli3 acts to constrain widespread dorsal expansion of intermediate cell types in the *schlei* mutant. Overall, our data are consistent with a model whereby the *schlei* mutation acts with the Gli genes to specify and define the domains of ventral neuronal cell types of the neural tube.

The *Schlei* gene is required to restrict Shh targets in the limb

schlei mutants were initially identified based on polydactyly, a common feature in mouse cilia mutants (May et al., 2005; Haycraft et al., 2007; Zeng et al., 2010) as well as human ciliopathies (Ansley et al., 2003; Kytölä et al., 2006; Singla et al., 2010). Shh signaling regulates the number and identity of digits (Riddle et al., 1993; Litingtung et al., 2002; Harfe et al., 2004) by mediating the balance of Gli3 activator and repressor forms (Hui and Joyner, 1993; Litingtung et al., 2002), whereas Gli1 and Gli2 are dispensable for digit patterning (Park et al., 2000; Bai et al., 2002). Since we identified Shh signaling anomalies in *schlei* neural tubes, we tested whether *schlei* mutant limbs might have similar patterning changes underlying the polydactyly phenotype. The expression of *Shh* ligand was normal (Fig. 5A,B); however, we found that its direct targets *Gli1* (Fig. 5C,D) and *Gremlin* (Fig. 5G,H) were anteriorly expanded in *schlei* limbs, suggesting a broadened response to Shh signaling. Occasionally (n=3/40), *schlei* mutant limbs displayed a discrete ectopic anterior spot of *Gli1* expression in addition to the expanded posterior domain (see Fig. S4 in supplemental material). Expression of *Ptch1*, an additional direct target of Hh signaling, appeared relatively normal in *schlei* mutants, suggesting that Shh targets are affected differentially (Fig. 5E,F). Thus, in contrast to mutants with a complete loss of cilia, in which *Gli1* and *Ptch1* expression are reduced or completely lost (Liu et al., 2005; May et al., 2005; Haycraft et al., 2007; Zeng et al., 2010), there appears to be an upregulation of the Shh pathway in *schlei*. This indicates that at least some *schlei* mutant cells can receive and respond to the Shh signal, despite the striking loss of cilia in the mutant limb.

The *schlei* mutation affects Gli3 function to regulate digit number, but not identity

In the limb, Shh acts primarily through the Gli3 transcription factor, and the functions of both Gli3A and Gli3R are essential for normal limb development (Wang et al., 2007). Cilia are required for normal processing of full-length Gli3 into Gli3R (Haycraft et al., 2005; Huangfu and Anderson, 2005; Liu et al., 2005), and for the transformation of full-length Gli3 to Gli3A. Complete loss of cilia in limb mesenchyme leads to multiple, unpatterned digits (Haycraft et al., 2007); however, the *schlei* mutant shows a milder, preaxial polydactyly phenotype (Figs 1, 6A,B). Therefore, we set out to test whether Gli3 processing was altered in *schlei* mutants. In contrast to other cilia mutants (Haycraft et al., 2005; Huangfu and Anderson, 2005; Liu et al., 2005; May et al., 2005; Zeng et al., 2010), we were unable to detect a difference in Gli3R or Gli3A levels in *schlei* mutant limbs as measured by Western blot (see Fig. S4 in supplementary material).

Although Gli3 processing and levels appeared normal, Western blots cannot reveal protein function. To test if the *schlei* mutation affects Gli3 function, we examined Shh targets in *schlei-Shh* double mutants. Our rationale was that in the absence of Shh, only Gli3R should be present and thus we should be able to detect if repressor function was altered in *schlei-Shh* animals. Strikingly, in contrast to the single digit that develops in *Shh* mutants ((Chiang et al., 1996); Fig. 6C), in the *schlei-Shh* double mutant, we observed a rescue of digit

number, with four to five digits forming on each double mutant limb, as marked by *Sox9* (Fig. 6D). To further investigate this rescue, we examined expression of *Gli1* and *Gremlin*, which are normally lost in *Shh* mutants (Zuniga et al., 1999; Chiang et al., 2001); Fig. 6E,G,I,K). *Gli1* expression, which was expanded in *schlei* mutants (Fig. 6F), was absent in *schlei-Shh* limbs (Fig. 6H). In contrast, *Gremlin* expression, which was also expanded in *schlei* limbs (Fig. 6J), was partially rescued in double mutants (Fig. 6L), suggesting that the repressive effects of Gli3R are relieved in double mutants.

Since extensive apoptosis occurs in *Shh* limbs ((Chiang et al., 2001); Fig. 6O), we hypothesized that the rescue of digit number in the *schlei-Shh* double mutant might be achieved through inhibition of this cell death. Indeed, loss of *schlei* resulted in a pronounced rescue of limb bud cell death as shown by TUNEL at e10.5 (Fig. 6P). Surprisingly, although loss of *schlei* function in a *Shh* mutant background rescued digit number, it did not rescue digit identity based on expression of *Hoxd11* (Fig. 6Q–T). Since *Hoxd11* marks posterior digits 2–5, the lack of *Hoxd11* expression combined with the short digit morphology demonstrated by the *Sox9* pattern suggests that the digits that form in *schlei-Shh* double mutants are all digit 1 (Dolle et al., 1989; Davis and Capecchi, 1994). These data demonstrate that the *schlei* mutation differentially affects Shh effectors to regulate distinct aspects of limb development like digit number (e.g. through *Gremlin*) and digit identity (e.g. through *Gli1*). Together, the morphology and gene expression of *schlei-Shh* double mutant limbs strongly resembles that of *Shh*^{-/-}; *Gli3*^{+/-} mutants (Litingtung et al., 2002). This suggests that loss of *schlei* may be analogous to reducing but not completely eliminating the function of Gli3R in the limb despite apparent normal Gli3 processing.

Identification of the causative mutation in *schlei*

Using meiotic recombination mapping we narrowed the genomic interval containing the *schlei* mutation to 1.88 Megabases on chromosome 11 containing 83 known or predicted transcripts (see Methods). To identify homozygous mutations in this region, we designed and utilized a Nimblegen Sequence Capture array (Hodges et al., 2007; Olson, 2007) followed by massively parallel Solexa sequencing (Bentley et al., 2008; D'Ascenzo et al., 2009). Using this method we identified 22 potential homozygous single nucleotide variants (SNVs; see Table S1 in supplementary material). We were able to eliminate most of these due to low read number, poor consensus score, or location within a repeat element. From the remaining SNVs, we focused on the only exonic mutation, located within the predicted four-pass *Transmembrane protein 107* (*Tmem107*) gene. We identified a single adenine to guanine transition in *Tmem107*, causing a change from a highly-conserved, negatively charged glutamic acid to a nonpolar glycine (E125G) within the fourth transmembrane domain (see Fig. S5 in supplementary material; Fig. 7A). This missense mutation was confirmed by standard sequencing in multiple independent *schlei* mutants. *Tmem107* is highly conserved within vertebrates, and although obvious orthologs have not been identified in *D. melanogaster*, they are present in *C. elegans*, *Nematostella* and *Chlamydomonas*, suggesting that *Tmem107* may have an ancient role in cilia regulation (see Fig. S6 in supplementary material). *Tmem107* is broadly expressed in the embryo ((Tang et al., 2010); see Fig. S5 in supplementary material) and *Tmem107* expressed sequence tags have been identified in juvenile and adult mouse tissues (NCBI; (Pontius et al., 2003)) indicating a potential postnatal role for *Tmem107*.

Mice homozygous for a targeted null allele of *Tmem107* (*Tmem107*^{tm1Lex}) have been previously described as embryonic lethal, but their phenotype has not been analyzed (Tang et al., 2010). To confirm that the *schlei* mutation in *Tmem107* underlies the mutant phenotype, we performed a complementation test with the *Tmem107*^{tm1Lex} allele. While *Tmem107*^{tm1Lex} heterozygotes appeared grossly normal (Fig. 7B,C), *schlei-Tmem107*^{tm1Lex} transheterozygotes failed to complement and developed preaxial polydactyly by e13.5 (Fig.

7D) and displayed a loss of the floorplate at e10.5 (Fig. 7E) similar to *schlei* homozygotes. Furthermore, these defects were also observed in *Tmem107^{tm1Lex/tm1Lex}* homozygous embryos, and defective neuronal patterning at the hindlimb level of the neural tube in these animals phenocopied that of *schlei* embryos (Fig. 7F,G; see Fig. S7 in supplemental material). Together these data confirm that the *schlei* mutant phenotype is caused by the E125G point mutation in *Tmem107*.

DISCUSSION

Cilia are dynamic organelles with essential functions in signaling, organogenesis, postnatal development and reproduction. Mutations in core cilia-building factors like the Kinesin motor subunits or IFT B complex proteins result in a complete loss of cilia (Marszalek et al., 1999; Rosenbaum and Witman, 2002). Experiments with these mutants have helped define which factors are essential for ciliogenesis and also how complete loss of cilia affects organogenesis and specific signaling pathways. In terms of Hh signaling, we now understand that the formation of GliR and the activation of full-length GliA require cilia (Haycraft et al., 2005; Huangfu and Anderson, 2005; Liu et al., 2005; May et al., 2005), although how cilia fulfill this role remains unresolved. One limitation to studying mutants with complete cilia loss is that the organelle being studied (i.e. the cilium) is absent. Thus, recent studies on mutants that, like *schlei*, still form some types of cilia (e.g. *Tctn1*, *Mks1*; (Reiter and Skarnes, 2006; Weatherbee et al., 2009; Garcia-Gonzalo et al., 2011)) are providing unique insights into the role of cilia in the development of specific tissues and signaling pathways.

Tmem107 is one of only a few transmembrane proteins known to play a role in cilia formation, and it is tempting to speculate that *Tmem107* may act within the ciliary membrane itself like *Tmem237* (Huang et al., 2011), at the transition zone like *Tmem216* (Valente et al., 2010; Garcia-Gonzalo et al., 2011), or both, like *Tmem67* (Smith et al., 2006; Garcia-Gonzalo et al., 2011). Although beyond the scope of this study, defining the specific roles of *Tmem107* in cilia formation and function should provide key insights into the role of cilia in development and disease.

***Tmem107* is essential for ciliogenesis and cilia-mediated signaling in a subset of embryonic tissues**

Cilia are required for common signaling pathways in multiple tissues (e.g. Hh) but also play distinct roles in specific organs. However, despite recent advances in understanding cilia function, it remains unclear what genes might contribute to making cilia in different tissues distinct. Using a forward genetics approach, we identified one of these factors, the novel transmembrane protein *Tmem107*. The *schlei* mutation in *Tmem107* modulates ciliogenesis and Shh signaling in multiple, but not all, tissues of the developing embryo, giving rise to a unique suite of ciliopathy features. *schlei* animals display polydactyly, microphthalmia, neural patterning defects and skeletal abnormalities common to cilia mutants. However, nodal cilia appear normal in *schlei* mutants and subsequently, no left-right defects develop (see Fig. S2 in supplementary material). Likewise, another typical feature of ciliopathies, cysts in the kidney and liver, also do not develop in *schlei* embryos (see Fig. S2 in supplementary material and data not shown). Finally, changes in Shh signaling in the neural tube show regional specificity in *schlei* mutants. Normally, Shh signaling from the notochord induces *Shh* in the floorplate throughout the embryo (Roelink et al., 1994; Roelink et al., 1995). However, in *schlei* mutants, *Shh* floorplate expression is lost in cervical and forelimb regions (Fig. 2) but still induced in the trunk. Together, these results suggest that *Tmem107* is differentially required for cilia formation and/or function in specific tissues within the embryo. This aspect of the *schlei* phenotype is similar to *Tctn1* mutants, which also show tissue-specific defects in ciliary assembly (Reiter and Skarnes,

2006; Garcia-Gonzalo et al., 2011). Thus far, we have demonstrated expression of *Tmem107* in all tissues examined, suggesting that the tissue specificity is the result of differential requirement for the gene product in different tissues, as opposed to spatially restricted expression. This raises the intriguing possibility that subsets of primary cilia have divergent composition and/or function, which could be one reason why ciliopathy phenotypes phenocopy Hh defects in some tissues (e.g. limb, neural tube), but have different etiologies in others. If specific populations of primary cilia depend upon distinct genes, this may also explain the spectrum of phenotypes observed across human ciliopathies.

The *schlei* mutation affects the function of Gli proteins

schlei mutants show distinct differences in Shh signaling compared to animals completely lacking cilia. In the neural tube, *schlei* embryos display reduced specification of high-level Shh targets (floorplate and V3) but also show an increased dorsal range of intermediate Shh targets (MN and V2). The fact that Shh-dependent cell types are still specified in *schlei* mutants indicates that Gli activator activity is functional despite the strong reduction in cilia. Specifically, Gli2 must still act as a positive mediator of Shh signaling in *schlei* mutants as *schlei-Gli2* embryos demonstrate a stronger loss of Shh signaling. The exacerbation of the dorsal expansion phenotype in *schlei-Gli3* double mutants also demonstrates that some repressive function of Gli3 is retained in *schlei* mutants. Thus, *schlei* mutant neural tubes appear to retain both Gli activator and repressor forms but with reduced function (Fig. 8).

In the limb, our Western blot analysis showed that anterior and posterior levels of full-length Gli3 and Gli3R are unaffected in *schlei* mutants. Shh targets are still expressed in *schlei* limbs, in contrast to complete cilia mutants (Liu et al., 2005; Haycraft et al., 2007), indicating that full-length Gli3 is a functional activator of the Shh pathway. However, the anterior expansion of Shh targets in *schlei* mutants and the derepression of *Gremlin* in *schlei-Shh* double mutants reveal that the function of Gli3R is compromised by the *schlei* mutation (Fig. 8). The morphology and gene expression patterns in *schlei-Shh* double mutant limbs strongly resemble those of *Shh^{-/-};Gli3^{+/-}* mutants (Litingtung et al., 2002) supporting the idea that the *schlei* mutation reduces the function of Gli3. Thus, similar to the neural tube, *schlei* mutant limbs appear to retain some GliR and GliA function despite the reduction in cilia number. This indicates that the few cilia that do form in *schlei* mutants maintain some ability to regulate Gli protein processing and functionality.

Forward genetics is a key approach to identify genes required for cilia form and function

Mutation discovery in human diseases has been greatly accelerated in recent years by the use of targeted enrichment and next-generation sequencing technologies (Bamshad et al., 2011; Ku et al., 2012). This study, along with a handful of others (Pyrgaki et al., 2011; Sheridan et al., 2011), has begun to apply the same principle to model systems. The result has been a dramatic decrease in the time it takes to progress from phenotype to affected gene, demonstrating that forward genetics screens in mice are a tractable and important avenue for gene discovery. In terms of cilia, bioinformatics and protein sequencing studies have identified hundreds of proteins in the cilium (Ostrowski et al., 2002; Avidor-Reiss et al., 2004; Pazour et al., 2005; Gherman et al., 2006), but determining which of these proteins are essential cilia factors is a daunting endeavor. However, this study and others highlight the immense potential of forward genetics approaches for identifying cilia genes (Huangfu et al., 2003; Garcia-Garcia et al., 2005; May et al., 2005; Liem et al., 2009; Weatherbee et al., 2009; Ko et al., 2010; Cui et al., 2011). Random mutagenesis provides an unbiased approach toward discovery of genes such as *Tmem107* that are critical for cilia biogenesis and function, but are not known components of well-studied pathways. Recent and future advances in high-throughput sequencing technology will continue to enhance our ability to

identify additional factors in the mouse that are critical regulators of development and disease.

Supplementary Material

Refer to Web version on PubMed Central for supplementary material.

Acknowledgments

We would like to thank Zhaoxia Sun for comments on the manuscript, Emily Mis, Sunjin Lee-Wölfel, Mustafa Khokha, and Martina Brueckner for helpful discussions, and William Horton and Stephanie Andrade for technical assistance. We also thank the Keck microarray resource at Yale for help with sequence capture, and the Yale Center for Cellular and Molecular Imaging for help with scanning electron microscopy.

FUNDING This work was supported by the National Institutes of Health [U01HD43478 to K.V. Anderson and L.A. Niswander; R01NS044385 to K.V. Anderson; R01HD32427 to L.A. Niswander; P30DK090744-01 Pilot & Feasibility funds to S.D. Weatherbee], the National Science Foundation [GRFP Fellowship to K.J. Christopher], and institutional startup funds from the Yale Genetics Department (S.D. Weatherbee).

REFERENCES

- Akiyama H, Chaboissier MC, Martin JF, Schedl A, de Crombrughe B. The transcription factor Sox9 has essential roles in successive steps of the chondrocyte differentiation pathway and is required for expression of Sox5 and Sox6. *Genes Dev.* 2002; 16(21):2813–28. [PubMed: 12414734]
- Ansley SJ, Badano JL, Blacque OE, Hill J, Hoskins BE, Leitch CC, Kim JC, Ross AJ, Eichers ER, Teslovich TM, et al. Basal body dysfunction is a likely cause of pleiotropic Bardet-Biedl syndrome. *Nature.* 2003; 425(6958):628–33. [PubMed: 14520415]
- Avidor-Reiss T, Maer AM, Koundakjian E, Polyanovsky A, Keil T, Subramaniam S, Zuker CS. Decoding cilia function: defining specialized genes required for compartmentalized cilia biogenesis. *Cell.* 2004; 117(4):527–39. [PubMed: 15137945]
- Bai CB, Auerbach W, Lee JS, Stephen D, Joyner AL. Gli2, but not Gli1, is required for initial Shh signaling and ectopic activation of the Shh pathway. *Development.* 2002; 129(20):4753–61. [PubMed: 12361967]
- Bai CB, Joyner AL. Gli1 can rescue the in vivo function of Gli2. *Development.* 2001; 128(24):5161–72. [PubMed: 11748151]
- Bamshad MJ, Ng SB, Bigham AW, Tabor HK, Emond MJ, Nickerson DA, Shendure J. Exome sequencing as a tool for Mendelian disease gene discovery. *Nat Rev Genet.* 2011; 12(11):745–55. [PubMed: 21946919]
- Bentley DR, Balasubramanian S, Swerdlow HP, Smith GP, Milton J, Brown CG, Hall KP, Evers DJ, Barnes CL, Bignell HR, et al. Accurate whole human genome sequencing using reversible terminator chemistry. *Nature.* 2008; 456(7218):53–9. [PubMed: 18987734]
- Caspary T, Garcia-Garcia MJ, Huangfu D, Eggenschwiler JT, Wyler MR, Rakeman AS, Alcorn HL, Anderson KV. Mouse Dispatched homolog 1 is required for long-range, but not juxtacrine, Hh signaling. *Curr Biol.* 2002; 12(18):1628–32. [PubMed: 12372258]
- Caspary T, Larkins CE, Anderson KV. The graded response to Sonic Hedgehog depends on cilia architecture. *Dev Cell.* 2007; 12(5):767–78. [PubMed: 17488627]
- Chiang C, Litingtung Y, Harris MP, Simandl BK, Li Y, Beachy PA, Fallon JF. Manifestation of the limb prepattern: limb development in the absence of sonic hedgehog function. *Dev Biol.* 2001; 236(2):421–35. [PubMed: 11476582]
- Chiang C, Litingtung Y, Lee E, Young KE, Corden JL, Westphal H, Beachy PA. Cyclopia and defective axial patterning in mice lacking Sonic hedgehog gene function. *Nature.* 1996; 383(6599):407–13. [PubMed: 8837770]
- Choi M, Scholl UI, Ji W, Liu T, Tikhonova IR, Zumbo P, Nayir A, Bakkaloglu A, Ozen S, Sanjad S, et al. Genetic diagnosis by whole exome capture and massively parallel DNA sequencing. *Proc Natl Acad Sci U S A.* 2009; 106(45):19096–101. [PubMed: 19861545]

- Cui C, Chatterjee B, Francis D, Yu Q, SanAgustin JT, Francis R, Tansey T, Henry C, Wang B, Lemley B, et al. Disruption of *Mks1* localization to the mother centriole causes cilia defects and developmental malformations in Meckel-Gruber syndrome. *Dis Model Mech*. 2011; 4(1):43–56. [PubMed: 21045211]
- D'Ascenzo M, Meacham C, Kitzman J, Middle C, Knight J, Winer R, Kukricar M, Richmond T, Albert TJ, Czechanski A, et al. Mutation discovery in the mouse using genetically guided array capture and resequencing. *Mamm Genome*. 2009; 20(7):424–36. [PubMed: 19629596]
- Dai P, Akimaru H, Tanaka Y, Maekawa T, Nakafuku M, Ishii S. Sonic Hedgehog-induced activation of the *Gli1* promoter is mediated by *GLI3*. *J Biol Chem*. 1999; 274(12):8143–52. [PubMed: 10075717]
- Davis AP, Capecchi MR. Axial homeosis and appendicular skeleton defects in mice with a targeted disruption of *hoxd-11*. *Development*. 1994; 120(8):2187–98. [PubMed: 7925020]
- Ding Q, Motoyama J, Gasca S, Mo R, Sasaki H, Rossant J, Hui CC. Diminished Sonic hedgehog signaling and lack of floor plate differentiation in *Gli2* mutant mice. *Development*. 1998; 125(14):2533–43. [PubMed: 9636069]
- Dolle P, Izpisua-Belmonte JC, Falkenstein H, Renucci A, Duboule D. Coordinate expression of the murine *Hox-5* complex homoeobox-containing genes during limb pattern formation. *Nature*. 1989; 342(6251):767–72. [PubMed: 2574828]
- Fliegaut M, Benzing T, Omran H. When cilia go bad: cilia defects and ciliopathies. *Nat Rev Mol Cell Biol*. 2007; 8(11):880–93. [PubMed: 17955020]
- Garcia-Garcia MJ, Eggenschwiler JT, Caspary T, Alcorn HL, Wyler MR, Huangfu D, Rakeman AS, Lee JD, Feinberg EH, Timmer JR, et al. Analysis of mouse embryonic patterning and morphogenesis by forward genetics. *Proc Natl Acad Sci U S A*. 2005; 102(17):5913–9. [PubMed: 15755804]
- Garcia-Gonzalo FR, Corbit KC, Sirerol-Piquer MS, Ramaswami G, Otto EA, Noriega TR, Seol AD, Robinson JF, Bennett CL, Josifova DJ, et al. A transition zone complex regulates mammalian ciliogenesis and ciliary membrane composition. *Nat Genet*. 2011; 43(8):776–84. [PubMed: 21725307]
- Gherman A, Davis EE, Katsanis N. The ciliary proteome database: an integrated community resource for the genetic and functional dissection of cilia. *Nat Genet*. 2006; 38(9):961–2. [PubMed: 16940995]
- Goetz SC, Anderson KV. The primary cilium: a signalling centre during vertebrate development. *Nat Rev Genet*. 2010; 11(5):331–44. [PubMed: 20395968]
- Goodrich LV, Milenkovic L, Higgins KM, Scott MP. Altered neural cell fates and medulloblastoma in mouse patched mutants. *Science*. 1997; 277(5329):1109–13. [PubMed: 9262482]
- Harfe BD. Keeping up with the zone of polarizing activity: New roles for an old signaling center. *Dev Dyn*. 2011; 240(5):915–9. [PubMed: 21360795]
- Harfe BD, Scherz PJ, Nissim S, Tian H, McMahon AP, Tabin CJ. Evidence for an expansion-based temporal *Shh* gradient in specifying vertebrate digit identities. *Cell*. 2004; 118(4):517–28. [PubMed: 15315763]
- Haycraft CJ, Banizs B, Aydin-Son Y, Zhang Q, Michaud EJ, Yoder BK. *Gli2* and *Gli3* localize to cilia and require the intraflagellar transport protein *polaris* for processing and function. *PLoS Genet*. 2005; 1(4):e53. [PubMed: 16254602]
- Haycraft CJ, Zhang Q, Song B, Jackson WS, Detloff PJ, Serra R, Yoder BK. Intraflagellar transport is essential for endochondral bone formation. *Development*. 2007; 134(2):307–16. [PubMed: 17166921]
- Hodges E, Xuan Z, Balija V, Kramer M, Molla MN, Smith SW, Middle CM, Rodesch MJ, Albert TJ, Hannon GJ, et al. Genome-wide in situ exon capture for selective resequencing. *Nat Genet*. 2007; 39(12):1522–7. [PubMed: 17982454]
- Houde C, Dickinson RJ, Houtzager VM, Cullum R, Montpetit R, Metzler M, Simpson EM, Roy S, Hayden MR, Hoodless PA, et al. *Hippi* is essential for node cilia assembly and Sonic hedgehog signaling. *Dev Biol*. 2006; 300(2):523–33. [PubMed: 17027958]
- Huang L, Szymanska K, Jensen VL, Janecke AR, Innes AM, Davis EE, Frosk P, Li C, Willer JR, Chodirker BN, et al. *TMEM237* is mutated in individuals with a Joubert syndrome related disorder

- and expands the role of the TMEM family at the ciliary transition zone. *Am J Hum Genet.* 2011; 89(6):713–30. [PubMed: 22152675]
- Huangfu D, Anderson KV. Cilia and Hedgehog responsiveness in the mouse. *Proc Natl Acad Sci U S A.* 2005; 102(32):11325–30. [PubMed: 16061793]
- Huangfu D, Liu A, Rakeman AS, Murcia NS, Niswander L, Anderson KV. Hedgehog signalling in the mouse requires intraflagellar transport proteins. *Nature.* 2003; 426(6962):83–7. [PubMed: 14603322]
- Hui CC, Joyner AL. A mouse model of greig cephalopolysyndactyly syndrome: the extra-toesJ mutation contains an intragenic deletion of the Gli3 gene. *Nat Genet.* 1993; 3(3):241–6. [PubMed: 8387379]
- Ingham PW, McMahon AP. Hedgehog signaling in animal development: paradigms and principles. *Genes Dev.* 2001; 15(23):3059–87. [PubMed: 11731473]
- Kasarskis A, Manova K, Anderson KV. A phenotype-based screen for embryonic lethal mutations in the mouse. *Proc Natl Acad Sci U S A.* 1998; 95(13):7485–90. [PubMed: 9636176]
- Ko HW, Norman RX, Tran J, Fuller KP, Fukuda M, Eggenschwiler JT. Broad-minded links cell cycle-related kinase to cilia assembly and hedgehog signal transduction. *Dev Cell.* 2010; 18(2):237–47. [PubMed: 20159594]
- Kong Y. Btrim: A fast, lightweight adapter and quality trimming program for next-generation sequencing technologies. *Genomics.* 2011; 98(2):152–3. [PubMed: 21651976]
- Ku CS, Cooper DN, Polychronakos C, Naidoo N, Wu M, Soong R. Exome sequencing: Dual role as a discovery and diagnostic tool. *Ann Neurol.* 2012; 71(1):5–14. [PubMed: 22275248]
- Kyttala M, Tallila J, Salonen R, Kopra O, Kohlschmidt N, Paavola-Sakki P, Peltonen L, Kestila M. MKS1, encoding a component of the flagellar apparatus basal body proteome, is mutated in Meckel syndrome. *Nat Genet.* 2006; 38(2):155–7. [PubMed: 16415886]
- Li H, Durbin R. Fast and accurate short read alignment with Burrows-Wheeler transform. *Bioinformatics.* 2009; 25(14):1754–60. [PubMed: 19451168]
- Li H, Handsaker B, Wysoker A, Fennell T, Ruan J, Homer N, Marth G, Abecasis G, Durbin R. The Sequence Alignment/Map format and SAMtools. *Bioinformatics.* 2009; 25(16):2078–9. [PubMed: 19505943]
- Liem KF Jr, He M, Ocbina PJ, Anderson KV. Mouse Kif7/Costal2 is a cilia-associated protein that regulates Sonic hedgehog signaling. *Proc Natl Acad Sci U S A.* 2009; 106(32):13377–82. [PubMed: 19666503]
- Litingtung Y, Chiang C. Specification of ventral neuron types is mediated by an antagonistic interaction between Shh and Gli3. *Nat Neurosci.* 2000; 3(10):979–85. [PubMed: 11017169]
- Litingtung Y, Dahn RD, Li Y, Fallon JF, Chiang C. Shh and Gli3 are dispensable for limb skeleton formation but regulate digit number and identity. *Nature.* 2002; 418(6901):979–83. [PubMed: 12198547]
- Liu A, Wang B, Niswander LA. Mouse intraflagellar transport proteins regulate both the activator and repressor functions of Gli transcription factors. *Development.* 2005; 132(13):3103–11. [PubMed: 15930098]
- Marszalek JR, Ruiz-Lozano P, Roberts E, Chien KR, Goldstein LS. Situs inversus and embryonic ciliary morphogenesis defects in mouse mutants lacking the KIF3A subunit of kinesin-II. *Proc Natl Acad Sci U S A.* 1999; 96(9):5043–8. [PubMed: 10220415]
- Matise MP, Epstein DJ, Park HL, Platt KA, Joyner AL. Gli2 is required for induction of floor plate and adjacent cells, but not most ventral neurons in the mouse central nervous system. *Development.* 1998; 125(15):2759–70. [PubMed: 9655799]
- May SR, Ashique AM, Karlen M, Wang B, Shen Y, Zarbalis K, Reiter J, Ericson J, Peterson AS. Loss of the retrograde motor for IFT disrupts localization of Smo to cilia and prevents the expression of both activator and repressor functions of Gli. *Dev Biol.* 2005; 287(2):378–89. [PubMed: 16229832]
- Nagy, A.; Gertsenstein, M.; Vintersten, K.; Behringer, R. *Manipulating the Mouse Embryo: A Laboratory Manual.* Cold Spring Harbor Laboratory Press; Cold Spring Harbor, NY: 2003.
- Nigg EA, Raff JW. Centrioles, centrosomes, and cilia in health and disease. *Cell.* 2009; 139(4):663–78. [PubMed: 19914163]

- Olson M. Enrichment of super-sized resequencing targets from the human genome. *Nat Methods*. 2007; 4(11):891–2. [PubMed: 17971778]
- Ostrowski LE, Blackburn K, Radde KM, Moyer MB, Schlatzer DM, Moseley A, Boucher RC. A proteomic analysis of human cilia: identification of novel components. *Mol Cell Proteomics*. 2002; 1(6):451–65. [PubMed: 12169685]
- Pan Y, Wang C, Wang B. Phosphorylation of Gli2 by protein kinase A is required for Gli2 processing and degradation and the Sonic Hedgehog-regulated mouse development. *Dev Biol*. 2009; 326(1):177–89. [PubMed: 19056373]
- Park HL, Bai C, Platt KA, Matisse MP, Beeghly A, Hui CC, Nakashima M, Joyner AL. Mouse Gli1 mutants are viable but have defects in SHH signaling in combination with a Gli2 mutation. *Development*. 2000; 127(8):1593–605. [PubMed: 10725236]
- Pazour GJ, Agrin N, Leszyk J, Witman GB. Proteomic analysis of a eukaryotic cilium. *J Cell Biol*. 2005; 170(1):103–13. [PubMed: 15998802]
- Persson M, Stamatakis D, te Welscher P, Andersson E, Bose J, Ruther U, Ericson J, Briscoe J. Dorsal-ventral patterning of the spinal cord requires Gli3 transcriptional repressor activity. *Genes Dev*. 2002; 16(22):2865–78. [PubMed: 12435629]
- Pontius, JU.; Wagner, L.; Schuler, GD. UniGene: a unified view of the transcriptome. In: McEntyre, J.; Ostell, J., editors. *The NCBI Handbook*. National Center for Biotechnology Information; Bethesda, MD: 2003.
- Pruitt KD, Harrow J, Harte RA, Wallin C, Diekhans M, Maglott DR, Searle S, Farrell CM, Loveland JE, Ruff BJ, et al. The consensus coding sequence (CCDS) project: Identifying a common protein-coding gene set for the human and mouse genomes. *Genome Res*. 2009; 19(7):1316–23. [PubMed: 19498102]
- Pyrgaki C, Liu A, Niswander L. Grainyhead-like 2 regulates neural tube closure and adhesion molecule expression during neural fold fusion. *Dev Biol*. 2011; 353(1):38–49. [PubMed: 21377456]
- Reiter JF, Skarnes WC. Tectonic, a novel regulator of the Hedgehog pathway required for both activation and inhibition. *Genes Dev*. 2006; 20(1):22–7. [PubMed: 16357211]
- Ribes V, Briscoe J. Establishing and interpreting graded Sonic Hedgehog signaling during vertebrate neural tube patterning: the role of negative feedback. *Cold Spring Harb Perspect Biol*. 2009; 1(2):a002014. [PubMed: 20066087]
- Riddle RD, Johnson RL, Laufer E, Tabin C. Sonic hedgehog mediates the polarizing activity of the ZPA. *Cell*. 1993; 75(7):1401–16. [PubMed: 8269518]
- Roelink H, Augsburger A, Heemskerk J, Korzh V, Norlin S, Ruiz i Altaba A, Tanabe Y, Placzek M, Edlund T, Jessell TM, et al. Floor plate and motor neuron induction by vhh-1, a vertebrate homolog of hedgehog expressed by the notochord. *Cell*. 1994; 76(4):761–75. [PubMed: 8124714]
- Roelink H, Porter JA, Chiang C, Tanabe Y, Chang DT, Beachy PA, Jessell TM. Floor plate and motor neuron induction by different concentrations of the amino-terminal cleavage product of sonic hedgehog autoproteolysis. *Cell*. 1995; 81(3):445–55. [PubMed: 7736596]
- Rohatgi R, Milenkovic L, Scott MP. Patched1 regulates hedgehog signaling at the primary cilium. *Science*. 2007; 317(5836):372–6. [PubMed: 17641202]
- Rosenbaum JL, Witman GB. Intraflagellar transport. *Nat Rev Mol Cell Biol*. 2002; 3(11):813–25. [PubMed: 12415299]
- Sasaki H, Nishizaki Y, Hui C, Nakafuku M, Kondoh H. Regulation of Gli2 and Gli3 activities by an amino-terminal repression domain: implication of Gli2 and Gli3 as primary mediators of Shh signaling. *Development*. 1999; 126(17):3915–24. [PubMed: 10433919]
- Sharma N, Berbari NF, Yoder BK. Ciliary dysfunction in developmental abnormalities and diseases. *Curr Top Dev Biol*. 2008; 85:371–427. [PubMed: 19147012]
- Sheridan R, Lampe K, Shanmukhappa SK, Putnam P, Keddache M, Divanovic S, Bezerra J, Hoebe K. Lampe1: An ENU-Germline Mutation Causing Spontaneous Hepatosteatoses Identified through Targeted Exon-Enrichment and Next-Generation Sequencing. *PLoS One*. 2011; 6(7):e21979. [PubMed: 21760938]
- Singla V, Romaguera-Ros M, Garcia-Verdugo JM, Reiter JF. Ofd1, a human disease gene, regulates the length and distal structure of centrioles. *Dev Cell*. 2010; 18(3):410–24. [PubMed: 20230748]

- Smith UM, Consugar M, Tee LJ, McKee BM, Maina EN, Whelan S, Morgan NV, Goranson E, Gissen P, Lilliquist S, et al. The transmembrane protein meckelin (MKS3) is mutated in Meckel-Gruber syndrome and the wpk rat. *Nat Genet.* 2006; 38(2):191–6. [PubMed: 16415887]
- Tanabe Y, Roelink H, Jessell TM. Induction of motor neurons by Sonic hedgehog is independent of floor plate differentiation. *Curr Biol.* 1995; 5(6):651–8. [PubMed: 7552176]
- Tang T, Li L, Tang J, Li Y, Lin WY, Martin F, Grant D, Solloway M, Parker L, Ye W, et al. A mouse knockout library for secreted and transmembrane proteins. *Nat Biotechnol.* 2010; 28(7):749–55. [PubMed: 20562862]
- Traiffort E, Angot E, Ruat M. Sonic Hedgehog signaling in the mammalian brain. *J Neurochem.* 2010; 113(3):576–90. [PubMed: 20218977]
- Valente EM, Logan CV, Mougou-Zerelli S, Lee JH, Silhavy JL, Brancati F, Iannicelli M, Travaglini L, Romani S, Illi B, et al. Mutations in TMEM216 perturb ciliogenesis and cause Joubert, Meckel and related syndromes. *Nat Genet.* 2010; 42(7):619–25. [PubMed: 20512146]
- Wang B, Fallon JF, Beachy PA. Hedgehog-regulated processing of Gli3 produces an anterior/posterior repressor gradient in the developing vertebrate limb. *Cell.* 2000; 100(4):423–34. [PubMed: 10693759]
- Wang C, Ruther U, Wang B. The Shh-independent activator function of the full-length Gli3 protein and its role in vertebrate limb digit patterning. *Dev Biol.* 2007; 305(2):460–9. [PubMed: 17400206]
- Weatherbee SD, Niswander LA, Anderson KV. A mouse model for Meckel syndrome reveals Mks1 is required for ciliogenesis and Hedgehog signaling. *Hum Mol Genet.* 2009; 18(23):4565–75. [PubMed: 19776033]
- Wijgerde M, McMahon JA, Rule M, McMahon AP. A direct requirement for Hedgehog signaling for normal specification of all ventral progenitor domains in the presumptive mammalian spinal cord. *Genes Dev.* 2002; 16(22):2849–64. [PubMed: 12435628]
- Zeng H, Hoover AN, Liu A. PCP effector gene Inturned is an important regulator of cilia formation and embryonic development in mammals. *Dev Biol.* 2010; 339(2):418–28. [PubMed: 20067783]
- Zuniga A, Haramis AP, McMahon AP, Zeller R. Signal relay by BMP antagonism controls the SHH/FGF4 feedback loop in vertebrate limb buds. *Nature.* 1999; 401(6753):598–602. [PubMed: 10524628]

The *schlei* mutation affects cilia number in a subset of developing mouse tissues.
schlei partially disrupts Gli activator and repressor function.

The *schlei* mutation acts downstream of Shh to control digit number but not identity.

The *schlei* mutation affects *Tmem107*, which encodes an ancient transmembrane protein.

Forward genetics plus sequence capture allows rapid discovery of developmental genes.

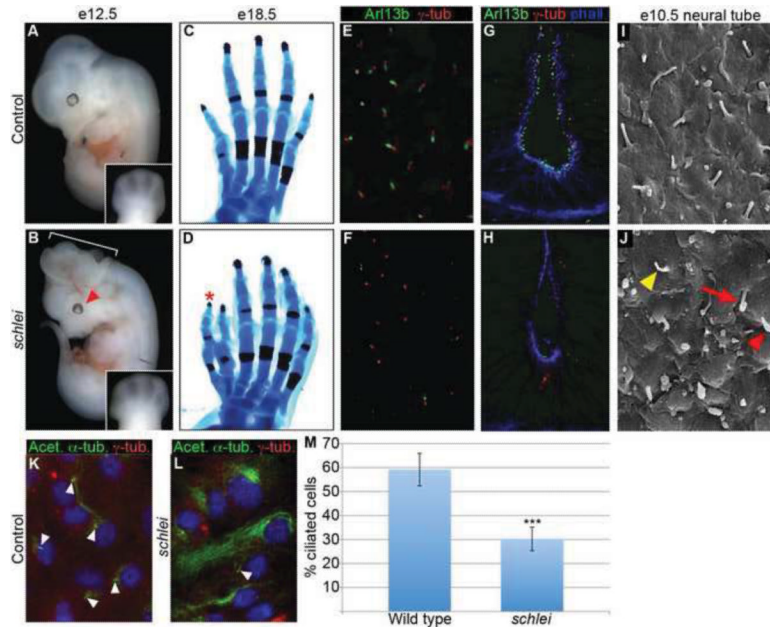


Figure 1. *schlei* mutants display multiple developmental defects and reduced primary cilia formation

e12.5 *schlei* mutant embryos display broadening of the limbs (A,B) and a subset of mutants also show exencephaly (60%; n=140; bracket in B) or microphthalmia (66% at e12.5 and older; n=29; arrowhead in B). Early limb broadening resolves into preaxial polydactyly (asterisk) as shown in e18.5 hindlimbs (C,D). Confocal Z-stack projections of immunostaining of transverse cryosections through the limb (E,F) and neural tube (G,H) at e11.5 reveals a reduction in cilia number (as marked by Arl13b in green) in *schlei* animals (F,H) as compared to wild type (E,G) despite the normal appearance and localization of basal bodies (as marked by γ -tubulin in red). (I,J) Scanning electron microscopy confirms a reduction in number of cilia in the neural tube of *schlei* animals (J) as compared to wild type (I). Cilia that do form in *schlei* are malformed, including examples with bulges at the tip (red arrowhead), elongated and curled cilia (red arrow), or thin cilia (yellow arrowhead). Differentiated MEFs from e13.5 wild type (K) and *schlei* (L) embryos immunostained using acetylated α -tubulin reveal a reduction in cilia number in the mutants (cilia, arrowheads). (M) *schlei* mutant MEF lines showed fewer cilia than wild-type (n=4 lines of each examined). On average, $59.14 \pm 6.75\%$ of wild type cells formed cilia, compared to $30.22 \pm 4.90\%$ of mutant cells ($p=0.00045$ by two-tailed student's t-test with equal variances). In (C,D) hindlimbs are visualized with Alizarin red (bone) and Alcian blue (cartilage) staining. Blue staining in (G,H) = phalloidin. Blue staining in (K,L) = DAPI. Control and *schlei* mutant images are shown at the same magnification.

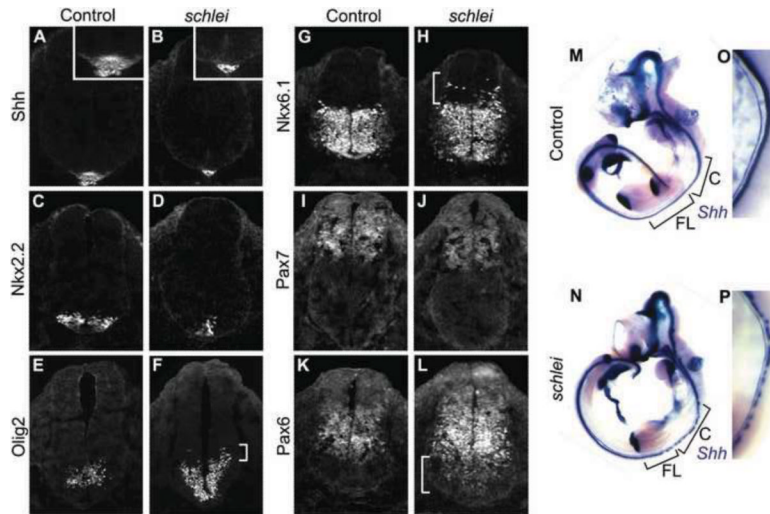


Figure 2. *schlei* mutants show disruptions in ventral cell type specification and neuronal subtype mixing in the neural tube

Sections through e10.5 neural tubes reveal that the floorplate is lost (A,B) and other ventral cell types including V3 interneuron progenitors (Nkx2.2+; C,D) are decreased in number and specified at more ventral locations than in wild type. Cells requiring intermediate levels of Shh signaling, such as motor neuron progenitors (Olig2+; E,F), are both specified more ventrally and expanded dorsally (bracket in F) in *schlei*. Other intermediate cell types, including a population marked by Nkx6.1 (G,H), are also expanded dorsally in the mutant and are mixed with more dorsal cell types (bracket in H). Some dorsal cell populations, such as the region demarcated by Pax7 expression, appear unchanged in *schlei* mutants (I,J). In contrast, Pax6 expression, which in wild type embryos (K) is inhibited by high levels of Shh, expands ventrally in *schlei* (bracket in L). The loss of the floorplate varies based on the axial level as visualized by whole mount *in situ* hybridization for *Shh*, with gaps in expression found particularly at the cervical and forelimb levels (M,N). (O,P) Higher magnification views of the cervical regions in e10.5 embryos highlight gaps in floorplate expression of *Shh* in *schlei* mutants. C; cervical; FL; forelimb. Control and *schlei* mutant images are shown at the same magnification.

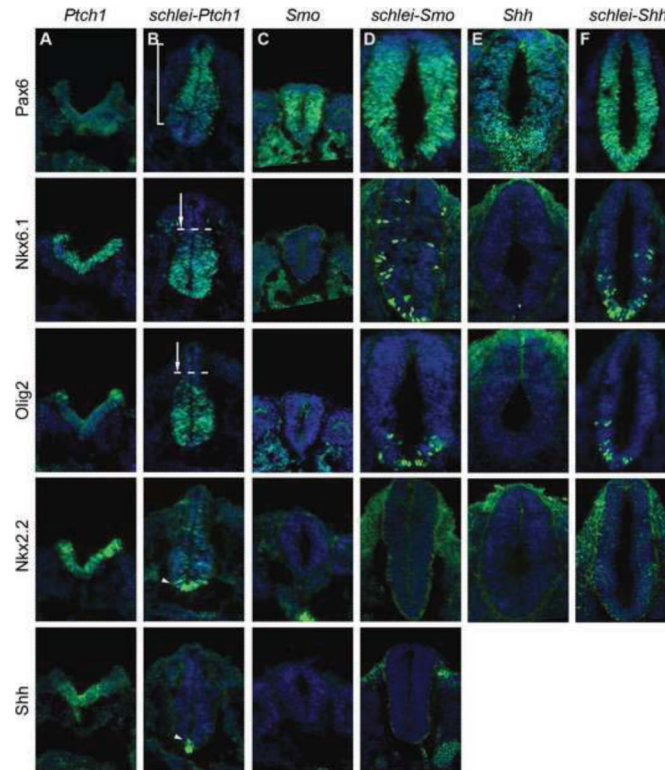


Figure 3. The *schlei* mutation rescues ventral neuronal specification in *Shh* pathway mutants
 e10.5 neural tubes stained for DAPI (blue) and neuronal markers (green). Expression of the dorsal marker Pax6, which is expanded in *Shh* (E) and *Smo* (C) mutants but absent in *Ptch1* (A) is rescued and dorsally restricted in *schlei-Ptch1* double mutants (B, bracket). In contrast, intermediate-level cells such as the Nkx6.1+ population and Olig2+ motor neuron progenitors, which require positive Shh signaling and are therefore absent in *Shh* and *Smo*, are able to form in *schlei-Shh* (F) and *schlei-Smo* (D) double mutants. These populations, which are expanded dorsally in *Ptch1*, are restored to a more ventral location in *schlei-Ptch1* double mutants (arrows). High-level Shh targets (Nkx2.2+ V3 interneuron progenitors and Shh+ floorplate cells) are expanded dorsally in *Ptch1* animals but are more ventrally restricted in *schlei-Ptch1* double mutants (arrowheads). However, *schlei* is not able to rescue the loss of these cell types in *Shh* and *Smo* mutants. All neural tube sections are shown at the same magnification.

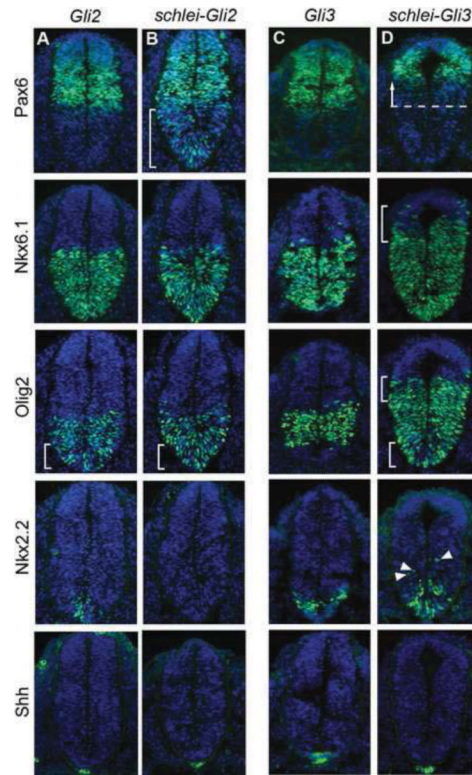


Figure 4. *schlei* interacts genetically with *Gli3* and *Gli2* to pattern the ventral and intermediate neural tube

e10.5 neural tubes stained for DAPI (blue) and neuronal markers (green). Expression of Pax6 is similar to wild type in *Gli2* (A) and *Gli3* (C) mutants, but the ventral border is extended ventrally in *schlei-Gli2* (B, bracket), consistent with the *schlei* single mutant. In *schlei-Gli3* embryos, there is a strong dorsal shift in the ventral border of Pax6 (D, arrow). The dorsal expansion of the Nkx6.1+ population observed in *schlei* is exacerbated in *schlei-Gli3* (bracket) but rescued in *schlei-Gli2*. While intermediate cells such as Olig2+ motor neuron progenitors are comparable to wild type in *Gli3* mutants, they are specified more ventrally in *Gli2*, *schlei-Gli2*, and *schlei-Gli3* (brackets). Additionally, the dorsal boundary of expression of Olig2+ is pushed even further dorsally in *schlei-Gli3* (upper bracket) than in *schlei*, but in *schlei-Gli2* is restored to a level similar to wild type. Nkx2.2+ V3 progenitor cells are reduced in number and specified more ventrally in *Gli2* mutants, but are completely lost in *schlei-Gli2* double mutants. Nkx2.2+ cells are normal in *Gli3*, but are specified more ventrally and dorsally (arrowheads) in *schlei-Gli3* double mutants. The floorplate, as marked by Shh, is normal in *Gli3* but is absent in *schlei-Gli3*, *Gli2*, and *schlei-Gli2* despite normal Shh staining in the notochord, similar to *schlei* mutants. All neural tube sections are shown at the same magnification.

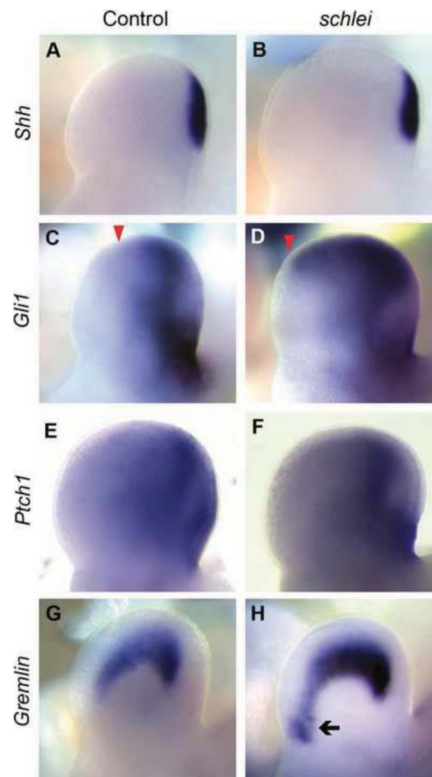


Figure 5. Shh signaling appears expanded in *schlei* mutant limbs at e11.5

Despite a normal domain of *Shh* (A,B), the boundary (arrowhead) of expression of *Gli1*, a direct target of Shh, is expanded anteriorly in *schlei* mutants (C,D). Note also the increased width of the mutant limb relative to the control, an early indication of polydactyly (visible in B,D). Expression of *Ptch1* appears unchanged in the mutant, suggesting differential sensitivities of various Shh targets (E,F). *Gremlin*, a downstream target of Shh activation, is expressed ectopically in a distinct region (arrow) in the anterior of the *schlei* limb (G,H). Control and *schlei* mutant images are shown at the same magnification.

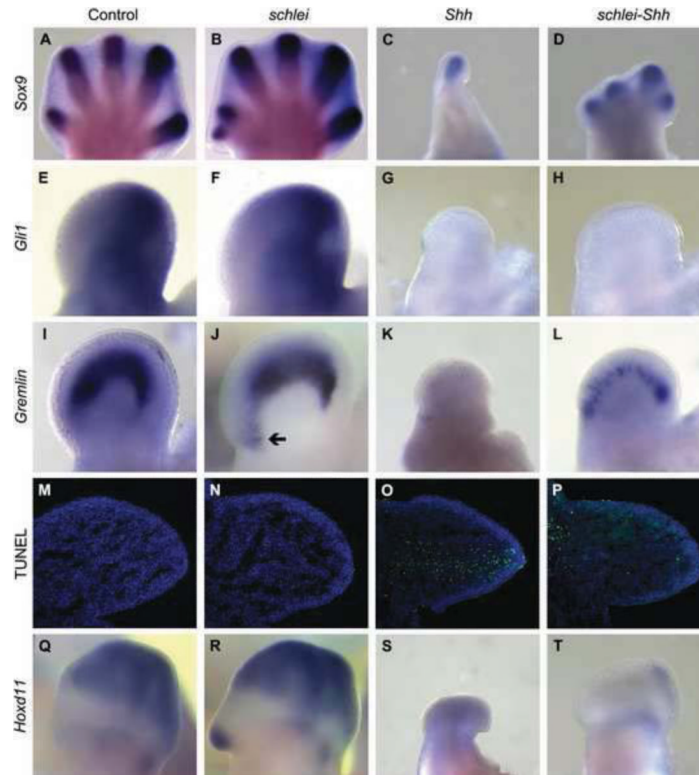


Figure 6. The *schlei* mutation partially rescues digit number in *Shh* mutant limbs
Sox9 marks condensing digits in e13.5 forelimbs (Akiyama et al., 2002), revealing five digits in wild type (A), an ectopic anterior digit in *schlei* mutants (B), a single digit in *Shh* mutants (C), and at least four digits in the double mutant (D). The direct positive target of *Shh*, *Gli1*, is not activated in *Shh* (G) or the double mutant (H), compared with the anterior expansion of expression observed in *schlei* (F) relative to wild type (E). However, expression of *Gremlin*, which is anteriorly expanded in *schlei* (arrow in J) as compared to wild type (I), is partially restored in the double mutant (L) despite its complete absence in the *Shh* mutant (K), suggestive of a loss of Gli3R function. The rescue of digit number in *schlei-Shh* double mutants may be due in part to a rescue of cell death; TUNEL (green staining) in e10.5 forelimb sections demonstrates that, similar to wild type (M) and *schlei* (N), double mutant limbs (P) lack the extensive distal cell death observed in *Shh* mutants (O). *Hoxd11* is expressed in the presumptive digits two through five in wild type (Q), and the ectopic digit in *schlei* variably expresses *Hoxd11*, indicating posterior identity in the example shown (R). *Hoxd11* is absent in both the *Shh* mutant (S) and the double mutant (T). Blue staining in M–P = DAPI. Control and *schlei* mutant images are shown at the same magnification.

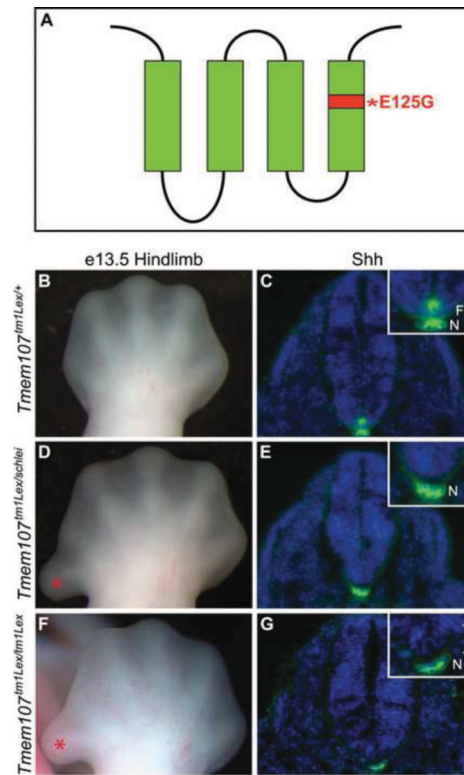


Figure 7. The *schlei* mutant phenotype results from a point mutation in *Tmem107*
 (A) Schematic representation of *Tmem107* protein, which is predicted to contain four transmembrane domains. Asterisk and red shading, location of the E125G missense mutation in *schlei* allele. Complementation analysis was carried out by crossing *Tmem107^{tm1Lex}* males with *schlei* females. At e10.5, transheterozygous embryos demonstrated that *Tmem107^{tm1Lex}* fails to complement *schlei* in anteroposterior limb patterning, as shown by preaxial polydactyly (asterisk) visible at e13.5 (B,D) and floorplate (FP) formation, as shown by staining for Shh (C,E). These phenotypes are also recapitulated in embryos homozygous for the *Tmem107^{tm1Lex}* mutant allele (F,G). Blue staining in (C,E,G) = DAPI. N = notochord. Brackets in E,G indicate loss of floorplate. Control, transheterozygotes, and homozygous mutant images are shown at the same magnification.

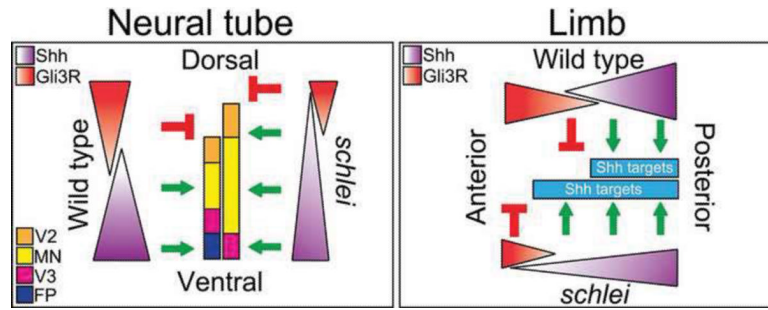


Figure 8. Model of Gli activity in the *schlei* mutant

In the neural tube, a ventral gradient of Shh signaling specifies ventral neuronal cell types, while dorsal Gli3R helps restrict the extent of their domain. In the *schlei* ventral neural tube, the highest level of Shh responsiveness is lost, but there is an increased range of intermediate-level signaling extending more dorsally, mimicking a shallower, but elongated gradient. Gli3 repressor function is also diminished in *schlei*, and together, this results in the absence of the highest-level ventral target, the floorplate (FP), combined with a broadened domain competent to form motor neurons (MN) and V2 interneurons. In the limb, a posterior gradient of Shh signaling specifies digit identity while anterior Gli3R restricts digit number. Similar to the neural tube, the Shh gradient appears extended in *schlei* limbs and together with decreased Gli3R function results in an expansion of Shh target gene expression (*Gremlin*, *Gli1*) in the anterior portion of the limb.